

# Comparative performance of LQG versus PID optimized by swarm approaches: a case study on a biomedical ventilation system

1<sup>st</sup> Alan Sovano Gomes  
*Institute of Technology*  
*Federal University of Pará*  
 Belém, Brazil  
 alan.s.gomes@ieee.org

2<sup>nd</sup> Walter Barra Jr.  
*Institute of Technology*  
*Federal University of Pará*  
 Belém, Brazil  
 walbarra@ufpa.br

3<sup>rd</sup> Antonio da Silva Silveira  
*Institute of Technology*  
*Federal University of Pará*  
 Belém, Brazil  
 asilveira@ufpa.br

4<sup>th</sup> Maria da Conceição Pereira Fonseca  
*Institute of Technology*  
*Federal University of Pará*  
 Belém, Brazil  
 conceicao@ufpa.br

5<sup>th</sup> Isabela Marques Miziara  
*Institute of Technology*  
*Federal University of Pará*  
 Belém, Brazil  
 immiziara@ufpa.br

**Abstract**—This paper compares the Linear Quadratic Gaussian (LQG) control method with the usage of swarm approaches in control systems, using as basis a paper that uses a mathematical model of an artificial ventilation system. The intent of this article is also to call attention to the good practices in control systems design, sometimes neglected by the researchers who seek to contribute to the field, but lack an appropriate theoretical background. In the presented case study, the classical LQG control shows equivalent result regarding the stability margins and temporal response when compared to a Proportional-Integral-Derivative (PID) controller that is tuned by three different swarm algorithms: Particle Swarm Optimization (PSO), Class Topper Optimization (CTO) and Constricted Class Topper Optimization (C-CTO). When the control signal is evaluated, the LQG controller clearly outperforms the other controllers. Final comments are made regarding some peculiarities of the basis paper and suggesting some orientations to better apply the presented swarm approaches and other nature-inspired optimization techniques in control systems design.

**Index Terms**—Control systems, LQG control, computational intelligence, artificial ventilation

## I. INTRODUCTION

Nature-inspired algorithms are being widely applied in control systems design. A quick search for scientific papers involving this topic can lead to the application of algorithms such as particle swarm optimization [1]–[6]; grey wolf optimizer [7]–[9]; and genetic algorithms [10]–[15], among others.

These algorithms, although very useful in a vast set of scenarios, can not be seen as “panacea” for all the control design problems, and must always be compared with well-established control techniques. The main problems that can be verified in some scientific papers that seek to apply the mentioned algorithms in control engineering are the absence of the control signal, the main product of a control system design [1], [3], [5], [6], [8], [13], [14]; and the lack of a discussion involving stability margins [1], [4], [5], [13], [15]. This information is essential from a control engineering point of view, in order to evaluate the real applicability of a

presented technique. If the control signal is not physically achievable, has abrupt changes that can damage the system being controlled and/or the closed-loop system has narrow stability margins, then the control system will be unfeasible. To evaluate these points, it is necessary not only to understand the system from a mathematical perspective, but from a physical one.

A lot of papers applying the mentioned techniques to design control systems propose an algorithm capable of tuning, in an optimal sense, the parameters of a Proportional-Integral-Derivative (PID) control [1]–[3], [5], [6], [8]–[11], [13]. These papers do not compare their proposed systems with the Linear Quadratic Gaussian (LQG) control, for example, that is a well-established technique with rigorous stability proofs and based on an optimization problem that takes into account not only the speed of convergence of the output, but also the energy spent in the process [16]. For a linear, well-conditioned system, the LQG control method results in a unique and optimal solution for a set of weighting matrices, that should be defined based on engineering intuition and knowledge of the proposed problem [17].

Both PID control tuned by nature-inspired algorithms, such as the Swarm Intelligence (SI) ones, and LQG control seek to achieve the same result: find an optimal solution to a specific problem. Why not, then, compare them both, to prove the benefits (or not) of these nature-inspired optimization techniques? Based on this question, this paper proposes a solution that uses the LQG method to control an artificial ventilation system, described in [1] and [18], where the authors of [1] proposed three SI-based techniques to tune a PID: Particle Swarm Optimization (PSO), which is based on the social behaviour of some species [19]; Class Topper Optimization (CTO), based on the competitive behaviour of students in a class [20]; and a modified Constricted Class Topper Optimization (C-CTO), which includes a constriction factor in the previous method, influencing the speed of

convergence of the algorithm [1].

The name "LQG" derives from the compensator's structure, which uses the estimation generated by a Kalman filter (also known as Linear Quadratic Estimator – LQE) and a deterministic Linear Quadratic Regulator (LQR) [17]. The LQG method results in a compensator structure that is defined by the procedure itself, and there are few tuning parameters that need to be used in the process, being a friendly design approach to complicated Multi-Input Multi-Output (MIMO) systems [21].

The layout of this paper is as follows. Section II describes the artificial ventilation system and the control problem associated with it. Section III presents the LQG control method, providing some theoretical background and the step-by-step design for the proposed problem. Section IV compares the LQG compensator with the SI-based PID controllers. Finally, section V presents some conclusions about the carried out study.

## II. SYSTEM MODELING AND PROBLEM DEFINITION

The mechanical ventilator is an electromedical equipment that is used to provide an adequate gas exchange to a patient that is not capable of doing it without assistance [22]. One of the ventilation modes present in this type of device is the Pressure-Controlled Ventilation (PCV). In PCV mode, the pressure in the air-ways,  $P_{aw}$ , must follow a preset reference signal, with the signal being a square wave where the maximum pressure value is the Positive Inspiratory Pressure (PIP) and the minimum value is the Positive End-Expiratory Pressure (PEEP) [18]. The PIP and PEEP values are defined by the clinicians, being based on pathological and physiological characteristics of the assisted patient.

The paper here analyzed [1] uses a simplified model to describe the ventilator-patient system in PCV mode, that was described in [18]. Basically,  $P_{aw}$  is influenced by a piston pump system that is actuated by an applied voltage  $U_a$  (in the mechanical ventilator side) and the lung mechanics (in the patient side). The lung mechanics are represented by a first-order system, which considers the respiratory system complacence and resistance in its model. The block diagram of this dynamic system is shown in Fig. 1, with the physical variables described in Table I.

From Fig. 1, it is possible to retrieve the following dynamic equations:

$$J_{eff}\dot{\omega} = -T_L + \Psi \frac{K_a}{1 + T_a s} U_a - \Psi^2 \frac{K_a}{1 + T_a s} - K_R \omega \quad (1)$$

$$T_L = K_M A_{piston}^2 \left( R_{rs} + \frac{1}{C_{rs} s} \right) \dot{z} \quad (2)$$

Using (1) and (2), it is possible to find the transfer function from  $U_a$  to  $P_{aw}$ . The parameters that were used in [1] to simulate the ventilator-patient dynamics in PCV mode were:  $K_a = 0.385 \text{ A/V}$ ,  $T_a = 9 \cdot e^{-5} \text{ seconds}$ ,  $\Psi = 2.96 \text{ N}\cdot\text{cm/A}$ ,  $J_{eff} = 0.0035 \text{ N}\cdot\text{cm}\cdot\text{s}^2$ ,  $A_{piston} = 1.65 \text{ dm}^2$ ,  $K_R = 0.005 \text{ N}\cdot\text{cm/rad}$ ,  $K_G = 0.4 \text{ mm/rad}$ ,  $R_{rs} = 5 \text{ mbar}\cdot\text{s/L}$ ,  $C_{rs} = 50 \text{ mL/mbar}$  and  $K_M = 0.0398 \text{ cm}$ .

Before proceeding, a note must be made. The dynamic model presented in [1] uses the described parameters as they

TABLE I  
MODEL PARAMETERS. ADAPTED FROM [1].

Parameter	Physical meaning
$U_a$	Applied voltage
$P_{aw}$	Air-ways pressure
$K_a$	Gain of current control loop of piston-drive system
$T_a$	Time constant of current control loop of piston-drive system
$\Psi$	Field flux linkage
$J_{eff}$	Moment of Inertia
$A_{piston}$	Piston area
$\dot{z}$	Piston speed
$z$	Piston position
$T_L$	Load torque
$K_R$	Friction coefficient
$K_G$	Transmission constant (motor revolutions to piston speed)
$R_{rs}$	Resistance of the respiratory system
$C_{rs}$	Complacence of the respiratory system
$\omega$	Angular velocity of the motor
$\dot{\omega}$	Angular acceleration of the motor
$K_M$	Transfer ration from $P_{aw}$ to $T_L$

are, that is, without correcting the parameters units. This results in the following transfer function:

$$\frac{P_{aw}(s)}{U_a(s)} = \frac{1074s + 4.298}{0.06064s^3 + 4.841s^2 + 1027s + 0.2477} \quad (3)$$

Equation (3) is an inconsistent dynamic model, since the units does not match. This indicates that, possibly, a lot of attention was given to the SI techniques, but not as much to the modeling part and its validation. From a control engineering perspective, the control system designer must always study the system to be controlled, in order to model it in an adequate way and, thus, properly control it. In the biomedical engineering field, the modeling part is very critical, as the designed system will interact with living people.

Since the controllers were designed for the wrong model, this nullifies the results of [1] regarding the mechanical ventilation system, but the techniques employed could still be used if the correct model is considered in the design. To show how the described mistake can considerably affect the system dynamics, consider the corrected model (with  $A_{piston}$  in  $\text{cm}^2$ ,  $K_G$  in  $\text{cm/rad}$  and  $C_{rs}$  in  $\text{L/mbar}$ ):

$$\frac{P_{aw}(s)}{U_a(s)} = \frac{1.074 \cdot 10^4 s + 3.298 \cdot 10^4}{0.06064s^3 + 3756s^2 + 7.79 \cdot 10^4 s + 2.477 \cdot 10^5} \quad (4)$$

A square-wave with a 2 seconds period and varying from 0 V to 1 V was applied as the input of (3) and (4), in order to

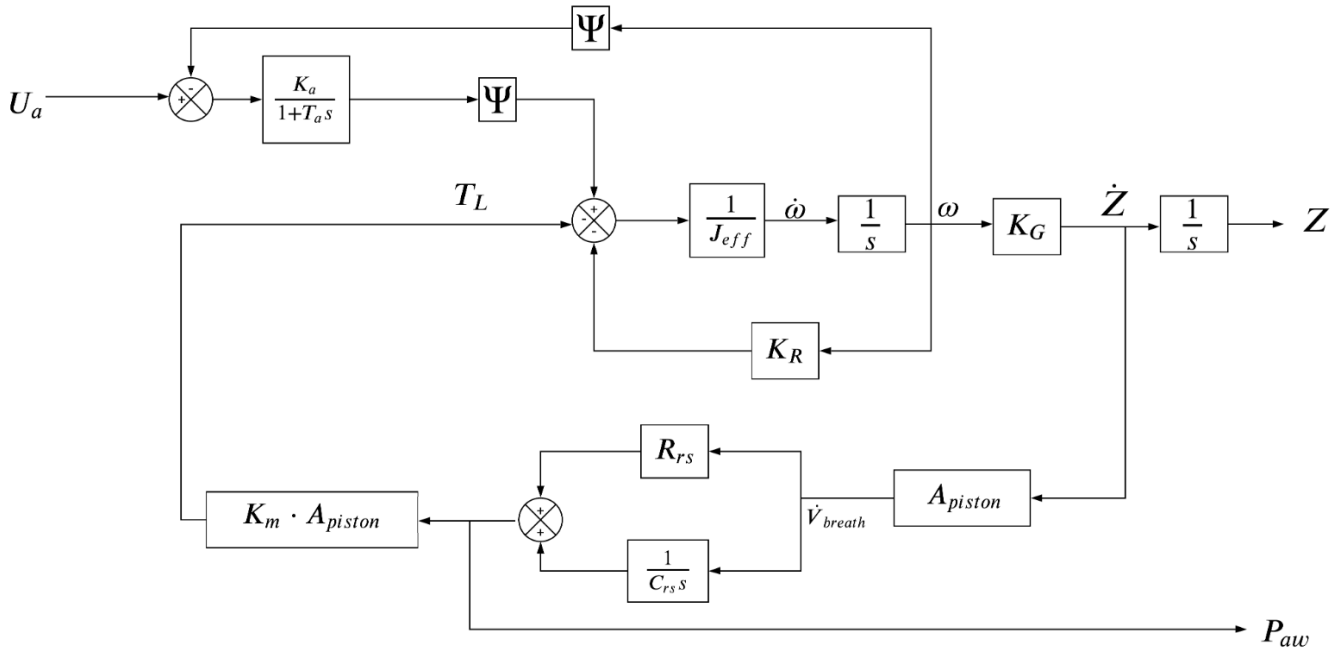


Fig. 1. Block diagram showing the relationship between  $U_a$  and  $P_{aw}$ , as described in [1], [18].

evaluate the dynamics in a scenario with a set-point change (from PEEP to PIP and then PIP to PEEP, periodically). The output of (3) is shown in Fig. 2, while the output of (4) is shown in Fig. 3. It is possible to conclude that the problems are entirely different: while [1] wrongly presents a system with oscillatory response and a static gain greater than one, the corrected system (with the correct units) presents a static gain significantly lower than one and a behaviour that shows no complex and conjugate poles.

Although an observation was made regarding the model in study, the following sections will discuss the project of a controller for the model described in (3), in order to have a standard to compare the SI-based PID from [1] with the LQG control method. The reader is advised to keep this information in mind from now on, until the end of the paper reading.

The primarily project's requirements that must be attended by the LQG controller, in order to compare it to the SI-based PID, were defined as:

- The system must track the square-wave input signal (a 1 V input must generate a 1 mbar output);
- It must have a null steady-state error;
- The oscillations in the system's output must be damped, with a maximum overshoot of 5%;
- The closed-loop performance must be compatible with the open-loop's speed response;
- The control signal must not contain any type of spikes.

This requirements define the control problem and, thus, the LQG controller can be designed, a process described in the next section.

### III. THE LQG CONTROL METHOD

#### A. Theoretical background

The LQG controller is synthesized with the connection of two subsystems: the Linear Quadratic Regulator (LQR) and

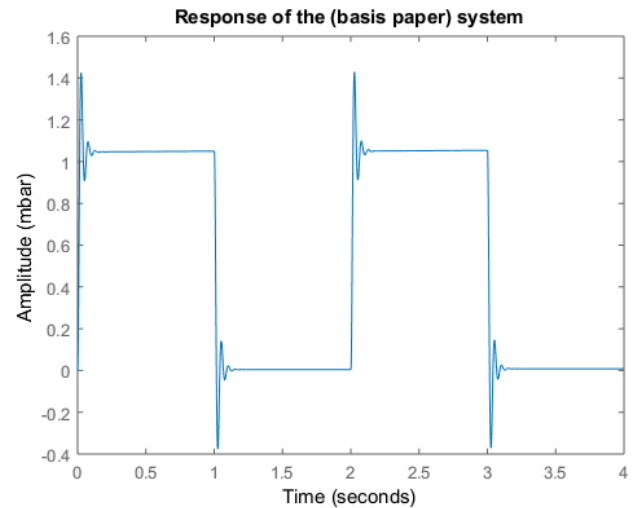


Fig. 2. Response of the system presented in [1] when a square-wave is applied at its input.

Linear Quadratic Estimator (LQE), also known as Kalman Filter [17]. Consider the general structure of a linear system described in state-space:

$$\dot{\mathbf{x}}(t) = A \cdot \mathbf{x}(t) + B \cdot \mathbf{u}(t) \quad (5)$$

$$\mathbf{y}(t) = C \cdot \mathbf{x}(t) + D \cdot \mathbf{u}(t) \quad (6)$$

The LQR problem can be formulated in terms of the states,  $\mathbf{x}(t)$ , and the control signal,  $\mathbf{u}(t)$ , through the following cost function [23]:

$$J_{LQR} = \frac{1}{2} \int_0^{\infty} [\mathbf{x}^T(t) Q \mathbf{x}(t) + \mathbf{u}^T(t) R \mathbf{u}(t)] dt \quad (7)$$

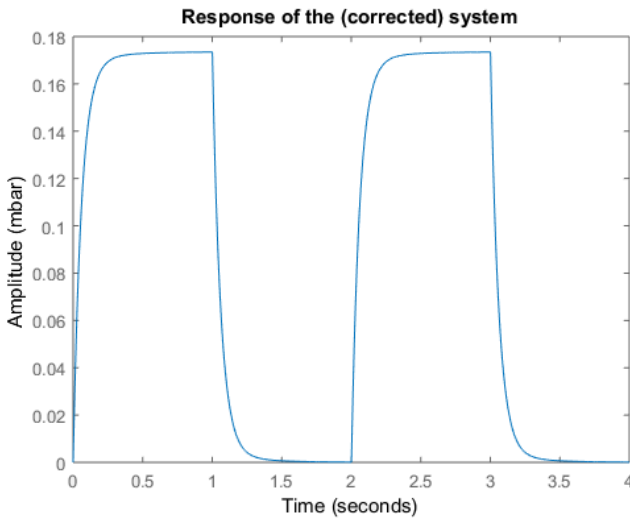


Fig. 3. Response of the (correct) system when a square-wave is applied at its input.

In (7),  $Q_{LQR}$  and  $R_{LQR}$  are weighting matrices, which must be defined by the designer according to some engineering criteria. While  $Q_{LQR}$  weights the speed of convergence of the states,  $R_{LQR}$  weights the energy spent to control the system (i.e., the control signal). The solution to this optimization problem comes from the continuous-time Algebraic Riccati Equation (CARE) [21]:

$$A^T P + PA - PBR^{-1}B^T P + Q = 0 \quad (8)$$

Matrix  $P$  is the solution to the CARE and also used to calculate the optimal state-feedback,  $K$ :

$$K = R^{-1}B^T P \quad (9)$$

The gain  $K$  is, then, the feedback gain that minimizes the cost function  $J_{LQR}$  in the LQR control problem.

In a state-space realization, usually one is not capable of measuring all the states, since it would require a lot of sensors to observe all these variables, and some of them may not even have physical meaning. To solve this problem, a Kalman Filter can be designed, which is capable of estimating the unmeasured states through the measured ones [21]. The Kalman Filter is the dual problem of the LQR, and can also be designed using (7), (8) and (9), but with the substitution of the matrices in the equation according to Table II [17]:

TABLE II  
DUALITY BETWEEN THE LQR AND THE KALMAN FILTER

LQR	$A$	$B$	$Q$	$R$	$P$	$K$
Kalman Filter	$A^T$	$C^T$	$Q_{kf}$	$R_{kf}$	$P_{kf}$	$L^T$

Where  $Q_{kf}$  and  $R_{kf}$  are weighting matrices for the Kalman Filter problem and  $L$  is the optimal estimation gain.

If we analyze the system described by (3), it is possible to observe that it does not have a natural integrator. For the system to follow a step-like reference with null steady-state error, an integrator must be included in the system [24]. This procedure, called “system augmentation”, is described in next.

## B. System augmentation by the addition of an integrator in the input

Consider the following augmented state vector:

$$\mathbf{x}_a(t) = \begin{bmatrix} y(t) \\ \dot{\mathbf{x}}(t) \end{bmatrix} \quad (10)$$

The state-space model presented in (5) and (6), considering the augmented state-vector and  $D = 0$ , can be rewritten in an augmented form as:

$$\dot{\mathbf{x}}_a(t) = \begin{bmatrix} 0 & C \\ \mathbf{0} & A \end{bmatrix} \cdot \mathbf{x}_a(t) + \begin{bmatrix} 0 \\ B \end{bmatrix} \cdot u_a(t) \quad (11)$$

$$y_a(t) = \begin{bmatrix} 1 & \mathbf{0} \end{bmatrix} \cdot \mathbf{x}_a(t) \quad (12)$$

This augmentation procedure adds an integrator to the input of the system, providing high gain at low frequencies and null steady-state error in closed-loop [25]. It is important to notice that the augmented control signal,  $u_a(t)$ , is the temporal derivative of the original control signal,  $u(t)$ :

$$u_a(t) = \dot{u}(t) \quad (13)$$

Although the input of the augmented system is  $u_a(t)$ , the control signal will, in fact, be  $u(t)$ . The matrices of the state-space realization of (3) used in the augmentation procedure are:

$$A = \begin{bmatrix} -79.84 & -132.3 & -0.1276 \\ 128 & 0 & 0 \\ 0 & 0.25 & 0 \end{bmatrix} \quad (14)$$

$$B = \begin{bmatrix} 16 \\ 0 \\ 0 \end{bmatrix} \quad (15)$$

$$C = \begin{bmatrix} 0 & 8.652 & 0.1384 \end{bmatrix} \quad (16)$$

$$D = 0 \quad (17)$$

Fig. 4 presents the frequency response of the studied system before and after the augmentation. The additional decay of 20 dB/decade in the magnitude response at low frequencies and the 90° lag in the phase response of the augmented system confirms that the integrator was successfully incorporated to the plant. Now, the system will have a null steady-state error in closed-loop for step-like reference signals.

## C. LQR design

After the augmentation procedure, the next step is to design the LQR. If the matrices  $Q$  and  $R$  are defined as identity matrices, the LQR will show a balanced compromise between performance and energy cost [21]. In the studied case,  $Q$  and  $R$  were defined as:

$$Q = \begin{bmatrix} 10000 & 0 & 0 & 0 \\ 0 & 1 & 0 & 0 \\ 0 & 0 & 1 & 0 \\ 0 & 0 & 0 & 1 \end{bmatrix} \quad (18)$$

$$R = 1 \quad (19)$$

The first element of the first row of matrix  $Q$  was multiplied by a factor of 10000, in order to increase the speed of

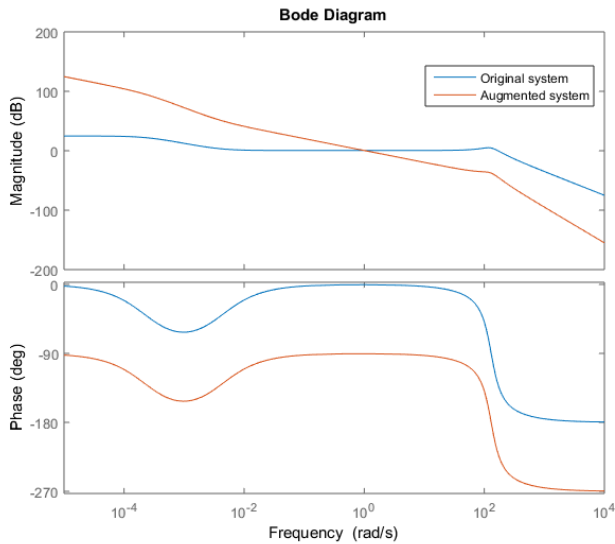


Fig. 4. Effects of the system's augmentation.

convergence (this element is related to the first state-variable, i.e., the output). That resulted in the following full state-feedback gain:

$$K = [ 100 \quad 6.5889 \quad 6.7606 \quad 0.2327 ] \quad (20)$$

For the system to track a unit step reference, the following control law must be adopted [24]:

$$u_a(t) = -K \cdot \mathbf{x}_a(t) + k_1 \cdot y_r(t) \quad (21)$$

In (21),  $k_1$  is the first element of  $K$  (the gain regarding the output variable) and  $y_r(t)$  is the reference signal for the output. For a control law like (21), the closed-loop state-space representation of the augmented system with full-state feedback is:

$$\dot{\mathbf{x}}_a(t) = (A_a - B_a K) \mathbf{x}_a(t) + B_a \cdot k_1 \cdot y_r(t) \quad (22)$$

$$\mathbf{y}_a(t) = [ 1 \quad \mathbf{0} ] \cdot \mathbf{x}_a(t) \quad (23)$$

Applying the reference square-wave signal to the system input generated the output response shown in Fig. 5. The output response presents an overshoot of 2%, and the system takes 0.03 seconds to go from zero to one for the first time.

To evaluate the system robustness, the closed-loop gain and phase margins were calculated, based on the peak values of the sensitivity and complementary sensitivity curves,  $M_S$  and  $M_T$ , respectively. The curves are shown in Fig. 6, and the margins were calculated using the following equations [26]:

$$GM_{dB} = 20 \cdot \log_{10} \left\{ \max \left[ \left( \frac{M_S}{M_S - 1} \right), \left( 1 + \frac{1}{M_T} \right) \right] \right\} \quad (24)$$

$$PM^\circ = \left( \frac{180^\circ}{\pi} \right) \cdot \max \left\{ \left[ 2 \cdot \sin^{-1} \left( \frac{1}{2 \cdot M_S} \right) \right], \left[ 2 \cdot \sin^{-1} \left( \frac{1}{2 \cdot M_T} \right) \right] \right\} \quad (25)$$

The usage of (24) and (25) results in a gain margin of 8.3 dB and a phase margin of 60°. According to [21], this system presents a good compromise between stability and

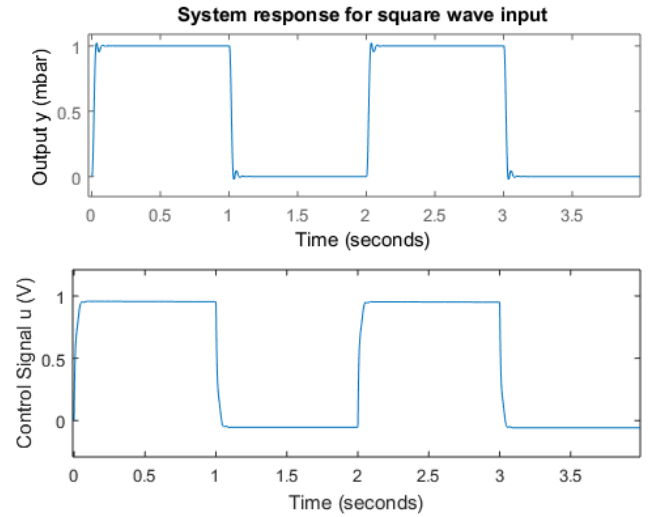


Fig. 5. Response of the closed-loop system with the LQR.

performance, since its margins are between 6 – 15 dB and 30° – 60°.

The LQR presents good temporal response and good stability margins, showing that an appropriate design has been achieved. It is possible now to proceed to the Kalman Filter design of the LQG compensator.

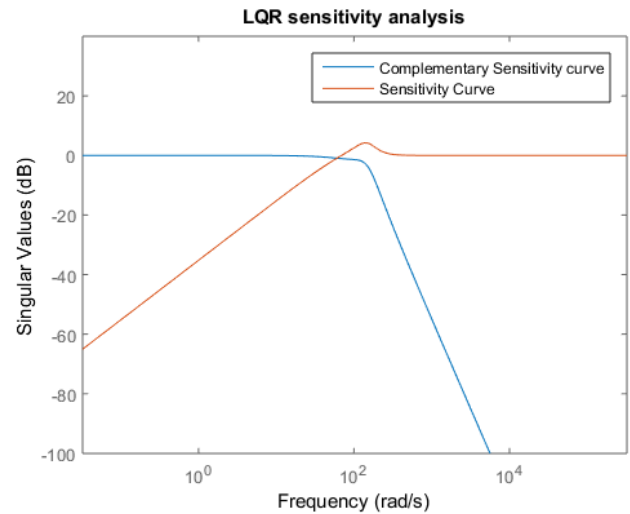


Fig. 6. Sensitivity and Complementary Sensitivity curves of the closed-loop system with the LQR.

#### D. Kalman Filter design

To design the Kalman Filter, the weighting matrices were defined as:

$$Q_{kf} = 10^7 \cdot I_{4 \times 4} \quad (26)$$

$$R_{kf} = 1 \quad (27)$$

In (26), the high multiplicative factor was used to increase the convergence of the estimation. These choices of  $Q_{kf}$  and  $R_{kf}$  resulted in the following estimation gain:

$$L^T = 10^3 \cdot [ 3.1635 \quad -0.1183 \quad 0.3905 \quad 3.1562 ] \quad (28)$$

To test the convergence of the filter's estimation, a reference signal can be applied to the closed-loop equation of the state observer [16]:

$$\hat{\dot{\mathbf{x}}}_a(t) = (A_a - LC_a)\hat{\mathbf{x}}_a(t) + B_a u(t) + L y_a(t) \quad (29)$$

$$\hat{\mathbf{y}}_a(t) = C_a \hat{\mathbf{x}}_a(t) \quad (30)$$

Where the use of the hat symbol ( $\hat{\cdot}$ ) denotes an estimation of the quantity of interest. To test the state observer, the input  $u(t)$  can be set to zero, in order to evaluate its behaviour when having access only to the system output.

In Fig. 7, it is possible to see the output of the filter when its input is the plant's output, showing the good performance of the estimation filter.

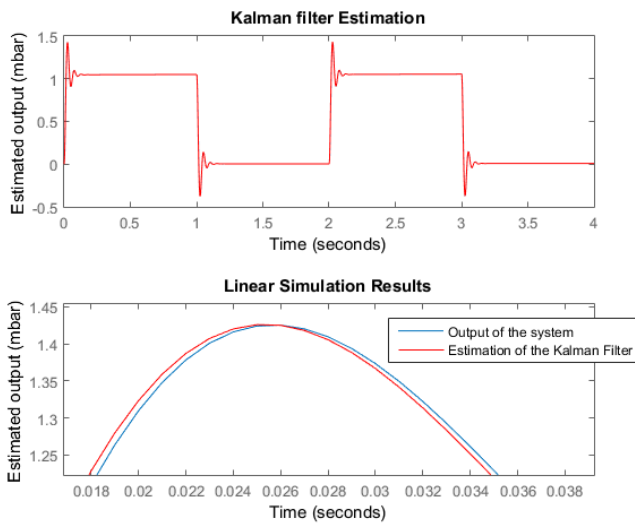


Fig. 7. Response of the Kalman Filter. A zoom was made in the first transitory to highlight its performance.

The calculated gain and phase margins of the Kalman filter were 6 dB and 60°, being also a robust system according to [21]. The sensitivity and complementary sensitivity curves of the system are shown in Fig. 8:

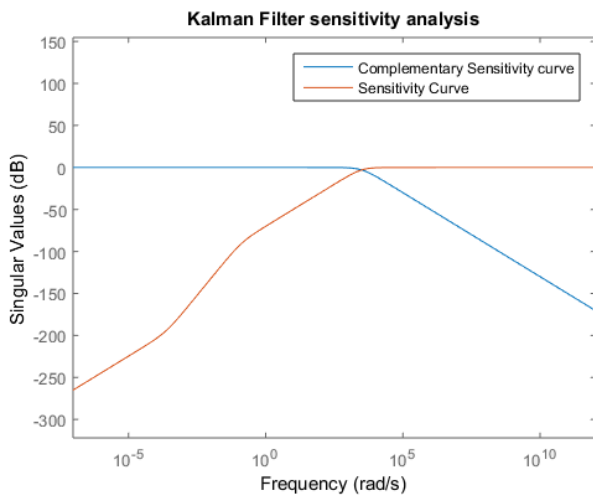


Fig. 8. Sensitivity and Complementary Sensitivity curves of the Kalman filter.

### E. LQG compensator design

Now that the LQR and the Kalman filter were designed, they can be interconnected to create the LQG controller. It is interesting to notice that the LQR and Kalman filter can be designed independently in order to obtain a LQG compensator, respecting the separation principle [27]. The closed-loop equations for both systems operating together are [16]:

$$\begin{bmatrix} \dot{\mathbf{x}}_a(t) \\ \hat{\dot{\mathbf{x}}}_a(t) \end{bmatrix} = \begin{bmatrix} A_a & -B_a K \\ LC_a & A_a - LC_a - B_a K \end{bmatrix} \begin{bmatrix} \mathbf{x}_a(t) \\ \hat{\mathbf{x}}_a(t) \end{bmatrix} + \begin{bmatrix} B_a \cdot k_1 \\ B_a \cdot k_1 \end{bmatrix} \cdot r(t) \quad (31)$$

$$\mathbf{y}(t) = \begin{bmatrix} C_a & \mathbf{0} \end{bmatrix} \begin{bmatrix} \mathbf{x}_a(t) \\ \hat{\mathbf{x}}_a(t) \end{bmatrix} \quad (32)$$

And the control law, based on the estimated states, is:

$$u_a(t) = -K \hat{\mathbf{x}}_a(t) + k_1 \cdot r(t) \quad (33)$$

The LQG compensator, in this case, obtained the same temporal characteristics of the LQR, shown in Fig. 5. The LQG system was also capable of retrieving the phase and gain margins of the LQR and, thus, its robustness. The sensitivity and complementary sensitivity curves of this system are the same that were shown in Fig. 6.

### IV. COMPARISON BETWEEN LQG AND SI-BASED PID CONTROLLERS

With the LQG compensator designed, its output response and control signal were compared to the three SI-based PID controllers. All responses are shown in Fig. 9, where a zoom in were made in order to compare the transitory response characteristics. It is possible to conclude that the LQG system presented a higher rising time when compared to the SI-based PID controllers, but in terms of the ventilator-patient system, this difference (of about 0.02 seconds) is neglectable. All systems presented an overshoot less than 10%, with the LQG controller being the system with minimal overshoot. Thus, all systems are comparable in respect to the closed-loop system's output.

In Fig. 10, the control signals of all four controllers are presented. The control signal of the SI-based controllers were not shown in [1], but could be plotted since the parameters of the PID were given. All the SI-based PID controllers presented high spikes in their control signal, which is an undesirable characteristic. That is caused by the derivative action of the PID controllers, which derivates the reference signal at the set-point changes, causing the spikes known as *derivative kicks* [28]. In a practical scenario, this kind of behaviour can damage the motor of the piston pump in the mechanical ventilator system, shortening its life cycle.

The phase and gain margins were also calculated for each system, as shown in Table III. All systems presented good stability margins according to the intervals presented in [21].

In order to quantify the performance of the controllers, the Integral Squared Error (ISE) and the Integral Squared of the Control Signal (ISU) were calculated. The indexes were obtained using a discrete approximation of the Integral Squared Signal (ISS), given by [29]:

$$ISS = \sum (\mathbf{w}^T \mathbf{w}) \cdot T_s \quad (34)$$

In (34),  $\mathbf{w}$  is an arbitrary signal and  $T_s$  is the sampling time used for the simulation of the systems. When  $\mathbf{w}$  is the error signal, ISS becomes ISE, and when  $\mathbf{w}$  becomes the control signal, ISS becomes ISU. The calculated values are shown in Table IV and the  $T_s$  used during the simulation was 0.001 s.

The values shown in Table IV confirm that the the PID controllers designed in [1] use a lot more energy than the LQG controller, but without a significant improvement.

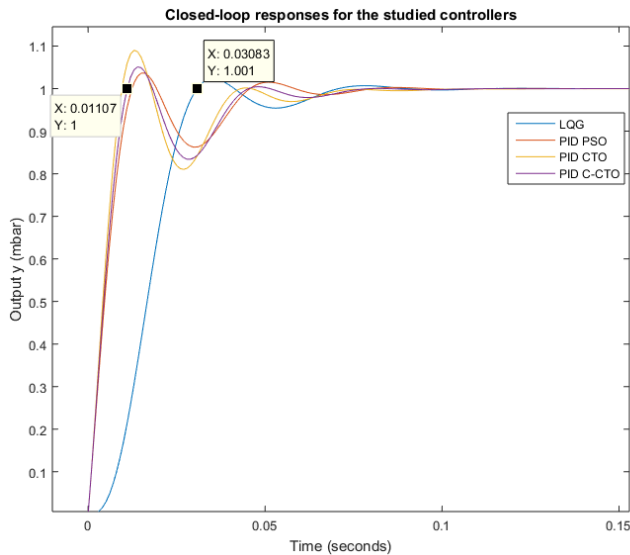


Fig. 9. Response of the closed-loop systems for the reference signal.

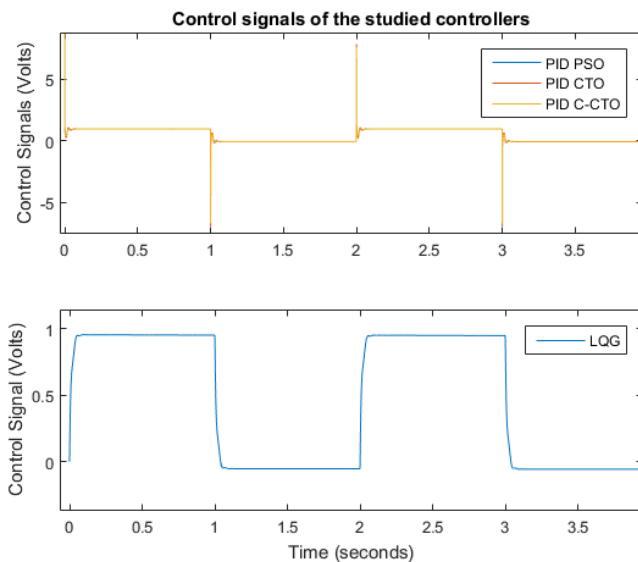


Fig. 10. Comparison between the control signals.

## V. CONCLUSIONS

This paper compared a LQG controller with three SI-based PID controllers designed for a mechanical ventilation system. It was possible to conclude that the controllers presented in [1] had a similar performance regarding the output signal characteristics when compared to the LQG compensator. All

TABLE III  
PHASE AND GAIN MARGINS OF THE STUDIED CONTROLLERS

Controller	Gain Margin (dB)	Phase margin (degrees)
PID PSO	16.5 dB	51.4°
PID CTO	12.2 dB	44.5°
PID C-CTO	14.7 dB	48.7°
LQG	8.3 dB	60°

TABLE IV  
ISE AND ISU FOR EACH CONTROLLER

Controller	ISE	ISU
PID PSO	0.0157	363.5991
PID CTO	0.0151	344.1776
PID C-CTO	0.0154	356.2718
LQG	0.0542	1.7965

controllers had good stability margins, but the control signal of the PID controllers suffered with spikes that could damage the electromedical equipment. Since the LQG controller signal was smoother, did not had any spikes and presented a significant lower ISU, the LQG compensator was considered more adequate to the studied problem.

In [1], the PID controller is presented in its ideal form, which, sometimes, is not even physically achievable and suffers from the *derivative kick* effect. A more reliable approach would be to consider the PID structure with a derivative filter, in order to limit the derivative action through a more limited frequency bandwidth [26]. The derivative action could be, also, approximated by a lead-lag term, in order to define where this effect should start and stop.

Another interesting topic to point out in [1] is that the objective function to be minimized by the swarm approaches is based only on the absolute error of the output over time. The LQG, on the other hand, considers both the output error and the control signal in its cost function, resulting in a more well-conditioned problem. If the swarm algorithms used a modified objective function, considering also the control effort, the controllers would probably use less energy to move the system's output (since the control effort would also be minimized). This way, the PID controllers would be compared more "fairly" with the LQG controller, since both would be based on similar minimization problems.

To conclude, it is important to highlight that the most problematic issues of [1] are regarding the control engineering and biomedical engineering areas. From the biomedical engineering point of view, the dynamic model is not described properly. Good knowledge about the model can lead the engineer to other types of designs for the control system, which could include an uncertainty in the respiratory system parameters and the application of adaptive, stochastic and robust control techniques. From the control engineering per-

spective, the problem was formulated ignoring the energy cost of the control signal, which is a critical issue when designing control systems. The SI techniques and other nature-inspired algorithms can and should be applied in control system design, but the designers must validate their studies and projects using pertinent and well consolidated evaluations, presented in classical papers of control systems engineering.

#### REFERENCES

- [1] D. Acharya and D. K. Das, "Swarm optimization approach to design pid controller for artificially ventilated human respiratory system," *Computer Methods and Programs in Biomedicine*, vol. 198, p. 105776, 2020.
- [2] H. Freire, P. M. Oliveira, and E. S. Pires, "From single to many-objective pid controller design using particle swarm optimization," *International Journal of Control, Automation and Systems*, vol. 15, no. 2, pp. 918–932, 2017.
- [3] J. Connor, M. Seyedmahmoudian, and B. Horan, "Using particle swarm optimization for pid optimization for altitude control on a quadrotor," in *2017 Australasian Universities Power Engineering Conference (AUPEC)*. IEEE, 2017, pp. 1–6.
- [4] L. Chen, S. Du, Y. He, M. Liang, and D. Xu, "Robust model predictive control for greenhouse temperature based on particle swarm optimization," *Information processing in agriculture*, vol. 5, no. 3, pp. 329–338, 2018.
- [5] M. M. Puralachetty and V. K. Pamula, "Differential evolution and particle swarm optimization algorithms with two stage initialization for pid controller tuning in coupled tank liquid level system," in *2016 International Conference on Advanced Robotics and Mechatronics (ICARM)*. IEEE, 2016, pp. 507–511.
- [6] T. Herlambang, D. Rahmalia, and T. Yulianto, "Particle swarm optimization (pso) and ant colony optimization (aco) for optimizing pid parameters on autonomous underwater vehicle (auv) control system," in *Journal of Physics: Conference Series*, vol. 1211, no. 1. IOP Publishing, 2019, p. 012039.
- [7] R.-E. Precup, R.-C. David, and E. M. Petriu, "Grey wolf optimizer algorithm-based tuning of fuzzy control systems with reduced parametric sensitivity," *IEEE Transactions on Industrial Electronics*, vol. 64, no. 1, pp. 527–534, 2016.
- [8] S. K. Verma, S. Yadav, and S. K. Nagar, "Optimization of fractional order pid controller using grey wolf optimizer," *Journal of Control, Automation and Electrical Systems*, vol. 28, no. 3, pp. 314–322, 2017.
- [9] J. Agarwal, G. Parmar, R. Gupta, and A. Sikander, "Analysis of grey wolf optimizer based fractional order pid controller in speed control of dc motor," *Microsystem Technologies*, vol. 24, no. 12, pp. 4997–5006, 2018.
- [10] J.-W. Perng and S.-C. Hsieh, "Design of digital pid control systems based on sensitivity analysis and genetic algorithms," *International Journal of Control, Automation and Systems*, vol. 17, no. 7, pp. 1838–1846, 2019.
- [11] A. Gupta, S. Goindi, G. Singh, H. Saini, and R. Kumar, "Optimal design of pid controllers for time delay systems using genetic algorithm and simulated annealing," in *2017 International Conference on Innovative Mechanisms for Industry Applications (ICIMIA)*. IEEE, 2017, pp. 66–69.
- [12] H. K. Tran and T. N. Nguyen, "Flight motion controller design using genetic algorithm for a quadcopter," *Measurement and Control*, vol. 51, no. 3–4, pp. 59–64, 2018.
- [13] T. Samakwong and W. Assawinchaichote, "Pid controller design for electro-hydraulic servo valve system with genetic algorithm," *Procedia Computer Science*, vol. 86, pp. 91–94, 2016.
- [14] H. Liang, J. Zou, K. Zuo, and M. J. Khan, "An improved genetic algorithm optimization fuzzy controller applied to the wellhead back pressure control system," *Mechanical Systems and Signal Processing*, vol. 142, p. 106708, 2020.
- [15] İ. Kaya and M. Nalbantoğlu, "Simultaneous tuning of cascaded controller design using genetic algorithm," *Electrical Engineering*, vol. 98, no. 3, pp. 299–305, 2016.
- [16] J. P. Hespanha, *Linear Systems Theory*. Princeton University Press, 2009.
- [17] J. J. Cruz, *Controle Robusto Multivariável*. edusp, 1996.
- [18] M. Walter and S. Leonhardt, "Control applications in artificial ventilation," in *2007 Mediterranean Conference on Control & Automation*. IEEE, 2007, pp. 1–6.
- [19] J. Kennedy and R. Eberhart, "Particle swarm optimization," in *Proceedings of ICNN'95-international conference on neural networks*, vol. 4. IEEE, 1995, pp. 1942–1948.
- [20] P. Das, D. K. Das, and S. Dey, "A new class topper optimization algorithm with an application to data clustering," *IEEE Transactions on Emerging Topics in Computing*, vol. 8, no. 4, pp. 948–959, 2018.
- [21] B. L. Stevens, F. L. Lewis, and E. N. Johnson, *Aircraft control and simulation: dynamics, controls design, and autonomous systems*, 3rd ed. John Wiley & Sons, 2015.
- [22] P. v. Platen, A. Pomprapa, B. Lachmann, and S. Leonhardt, "The dawn of physiological closed-loop ventilation—a review," *Critical Care*, vol. 24, pp. 1–11, 2020.
- [23] R. F. Stengel, *Optimal control and estimation*. Courier Corporation, 1994.
- [24] K. Ogata, *Modern control engineering*. New Jersey, USA: Prentice hall, 2010.
- [25] L. Castro, L. Cunha, B. Dutra, and A. Silveira, "Digital lqg controller design applied to an electronic system," *IEEE Latin America Transactions*, vol. 18, no. 03, pp. 581–588, 2020.
- [26] S. Skogestad and I. Postlethwaite, *Multivariable feedback control: analysis and design*, 2nd ed. John Wiley & Sons, 2005.
- [27] C.-T. Chen, *Linear System Theory and Design*. Princeton University Press, 1999.
- [28] A. Visioli, *Practical PID control*. Brescia, Italy: Springer Science & Business Media, 2006.
- [29] A. Silveira, R. Trentini, A. Coelho, R. Kutzner, and L. Hofmann, "Generalized minimum variance control under long-range prediction horizon setups," *ISA transactions*, vol. 62, pp. 325–332, 2016.